Int J Adv Manuf Technol (2017) 91:3635–3652
DOI 10.1007/s00170-017-0032-8

ORIGINAL ARTICLE

A flank correction face-milling method for bevel gears using a five-axis CNC machine

Yi-Pei Shih[1] · **Zi-Heng Sun**[1] · **Kuei-Li Lai**[1]

Received: 18 October 2016 / Accepted: 9 January 2017 / Published online: 27 January 2017

Abstract Face milling is extremely popular in industrial mass production of spiral bevel and hypoid gears because of its high productivity and the superior contact performance of the gear pairs it produces. This method, however, includes many cutting systems that must be implemented on numerous dedicated traditional machines with differently designed mechanisms. The five-axis CNC machine, in contrast, has enough degrees of freedom to handle all these cutting systems. As a result, the use of a general five-axis machine to produce face-milled bevel gears is attracting growing attention because it is so much more flexible than dedicated machines in small-scale diverse production. This paper therefore proposes a face-milling system with flank correction for bevel gears on a five-axis CNC machine. First, a mathematical model of the tooth surface is established based on a trunnion table type machine, after which the five coordinates of the five-axis machine are derived using the machine settings of a virtual cradle type bevel gear cutting machine. These five coordinates are degenerated to a function of the generating angle, and each coordinate is approximated as a polynomial in a Maclaurin series. Because flank topographic errors can be systematically reduced by adjusting the polynomial coefficients, a flank correction technology is developed based on a sensitivity analysis that investigates flank topographic deviations in terms of changes in coefficients. Based on this sensitivity matrix and the tooth surface errors measured, corrections are made to the five-axis coefficients using the least squares method. Finally, following a program accuracy check using NC verification software, several cutting experiments are performed to verify the correctness of the mathematical models.

Keywords Bevel gear · Face milling · Five-axis machine · Flank correction method

✉ Yi-Pei Shih
shihyipei@mail.ntust.edu.tw

Zi-Heng Sun
m10303126@mail.ntust.edu.tw

Kuei-Li Lai
kevin@minchen.com.tw

[1] Department of Mechanical Engineering, National Taiwan University of Science and Technology, No. 43, Sec. 4, Keelung Rd, Taipei 106, Taiwan, Republic of China

1 Introduction

Face milling (FM) and face hobbing (FH), the two primary methods used in the industrial mass production of spiral bevel and hypoid gears, have for decades been implemented on dedicated bevel gear cutting machines, which require numerous complex features such as cradle, helical motion, and modified roll ratio mechanisms. The modern CNC bevel gear cutting machine, in contrast, is a six-axis structure with enough degrees of freedom to handle for all cutting systems. Basically, this machine has five-axis synchronous interpolation for FM cutting systems and an additional electric gear box that enables synchronized movement in the cutter and workpiece rotation axes of FH cutting systems. FM gears can also be produced, however, on a general type five-axis machine, a highly feasible option whose low cost and flexibility in small-scale diverse production have prompted increasing attention. Five-axis machines may have three types of constructions: trunnion-table type (two rotation axes in table side), rotary-table and swivel-head type, or tilting head (two rotation axes in head side). The first two, which have a rotary workpiece table, are particularly suitable for machining gear tooth surfaces; however, even though several applications of these

machines have been introduced into industry, their technical details—in particular, their mathematical models—have not been revealed because of commercial considerations.

The mathematical models of bevel gear tooth surfaces, in contrast, are widely available in the literature, being most commonly based on a virtual cradle type bevel gear cutting machine. The first complete mathematical models of FM hypoid gears were established by Litvin and Gutman [1–3] using formate and helixform methods. Litvin et al. [4] then derived the machine settings for bevel gears using a cutter tilting method. Somewhat later, Fong [5] proposed a universal mathematical model for FM bevel gears that involves all supplemental motions for flank modification, and Shih et al. [6] then established a universal mathematical model for FH bevel gears. These models successfully improve gear pair contact performance at the design stage and enable the derivation of machine settings for all types of real-world cutting machines. More recently, Deng et al. [7] proposed an application for bevel gear production on a five-axis machine in which a disk cutter replaces an FM cutter head to provide greater flexibility in manufacturing large size gears. This method, however, has lower productivity. Shih et al. [8] also derived the coordinates for a trunnion table type five-axis machine from universal machine settings but without considering flank correction. Shih and Fong [10] also applied the bevel gear flank correction method developed by Litvin and Fuentes [9] for traditional machines on a modern CNC bevel gear cutting machine. Its application on a five-axis machine, however, has not yet been reported.

This paper therefore develops a mathematical model of flank correction for FM bevel gears on a five-axis machine by first deriving the five-axis coordinates as separate functions of a cradle angle approximated by a Maclaurin series. This derivation allows the cutting motion to be changed by adjusting these coefficients to reduce flank errors. A sensitivity matrix of the tooth surface coefficients is then determined that, when combined with measures of the flank topographic errors, enables least squares estimation of the five axes' corrective coefficients for minimizing deviations. Lastly, after an NC (VERICUT) verification is performed to simulate the correctness of the CNC data, several cutting experiments are conducted to verify the correctness of the mathematical models. The produced gear workpieces are shown in Fig. 1.

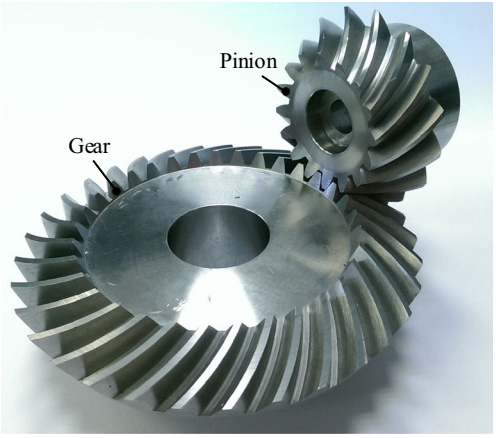

Fig. 1 Produced gear workpieces

2 Mathematical model of FM bevel gears based on a virtual cradle type bevel gear cutting machine

As previously emphasized, the virtual cradle type bevel gear cutting machine has adequate degrees of freedom to simulate the motion of bevel gear cutting using all types of FM and FH cutting methods. Hence, according to the motions for cutting a gear given by the virtual machine, traditional machines use additional mechanisms for cradle generation or the several supplemental motions (e.g., cutter tilt, helical motion, modified roll) that these latter require for a generating process and flank modification. FM cutting methods use FM cutter heads for the mass production of bevel gears because of their high precision and productivity. In this method, a plurality of inner (IB) and outer (OB) cutting blades are mounted alternately on a cutter head (see Fig. 2). The blade edge profile can be straight lined or circular, which latter achieves profile crowning for better contact performance. Here, the profile angle is represented by parameter α_b, the fillet radius by ρ_b, the cutter radius by r_0, the nominal cutter radius by r_c, the cutter height parameter by H_t, and the tool rotation angle by β. The cutter profile for the example gear pair and the adopted cutter are shown in Figs. 6 and 10, respectively.

If the blade edge is a straight line ($\mathbf{r}_a^{(l)}$) with a circular arc tip fillet ($\mathbf{r}_a^{(f)}$), its position vector is

$$\begin{cases} \mathbf{r}_a^{(l)}(u) = \left[x_a^{(l)}(u) \;\; 0 \;\; z_a^{(l)}(u) \;\; 1\right]^T \\ \mathbf{r}_a^{(f)}(u) = \left[x_a^{(f)}(u) \;\; 0 \;\; z_a^{(f)}(u) \;\; 1\right]^T \end{cases}, \quad \begin{cases} x_a^{(l)}(u) = \pm u\sin\alpha_b \\ z_a^{(l)}(u) = u\cos\alpha_b \end{cases}, \quad \begin{cases} x_a^{(f)}(u) = \pm\left(x_{cf} - \rho_b\cos u\right) \\ z_a^{(f)}(u) = z_{cf} + \rho_b\sin u \end{cases} \tag{1}$$

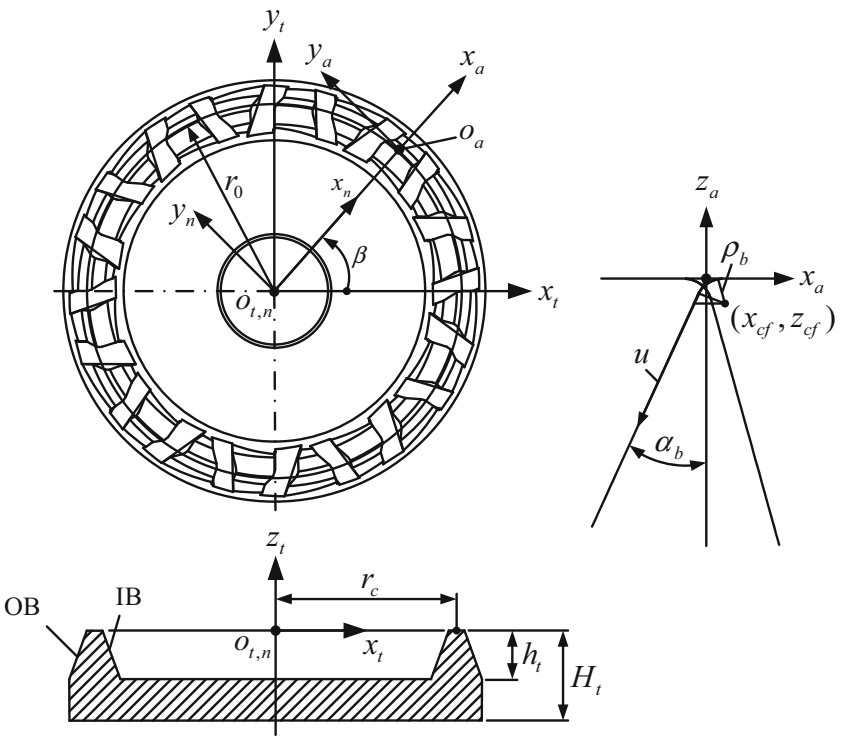

Fig. 2 Coordinate systems for an FM cutter head

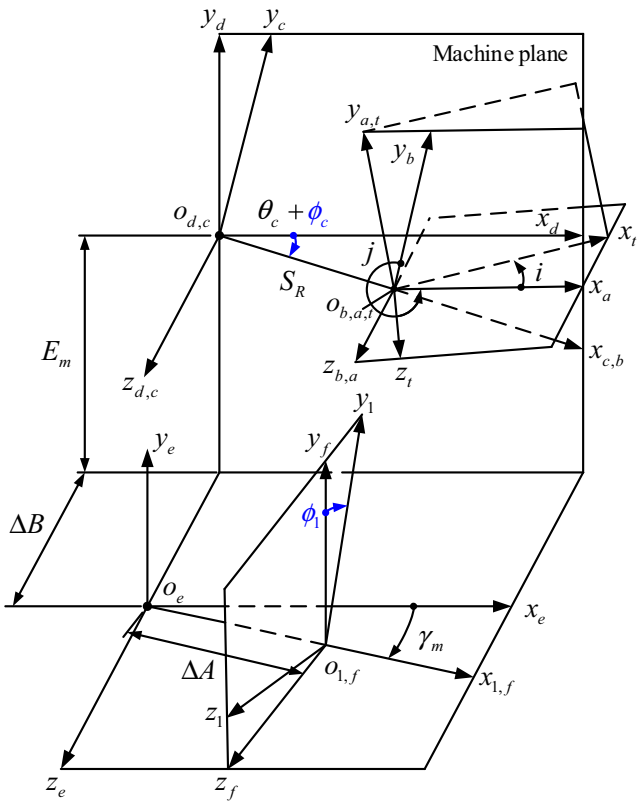

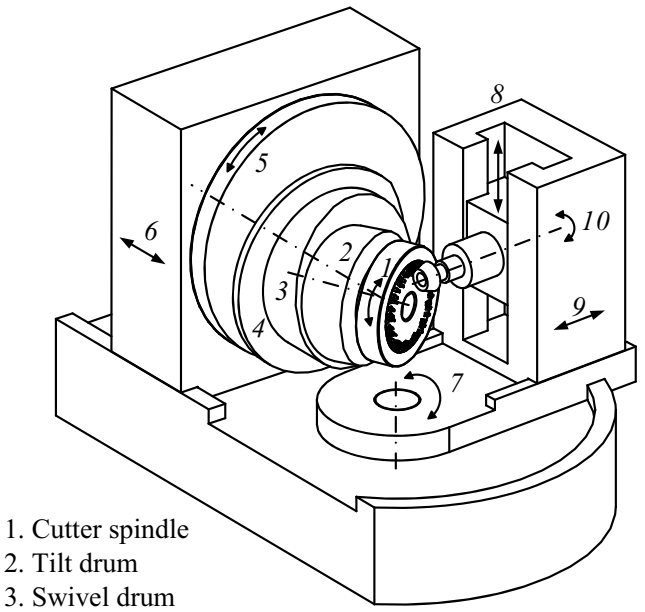

1. Cutter spindle
2. Tilt drum
3. Swivel drum
4. Eccentric drum
5. Cradle
6. Sliding base
7. Machine root angle
8. Blank offset
9. Machine center to back
10. Work spindle

Fig. 3 Coordinate systems of a virtual cradle type bevel gear generator

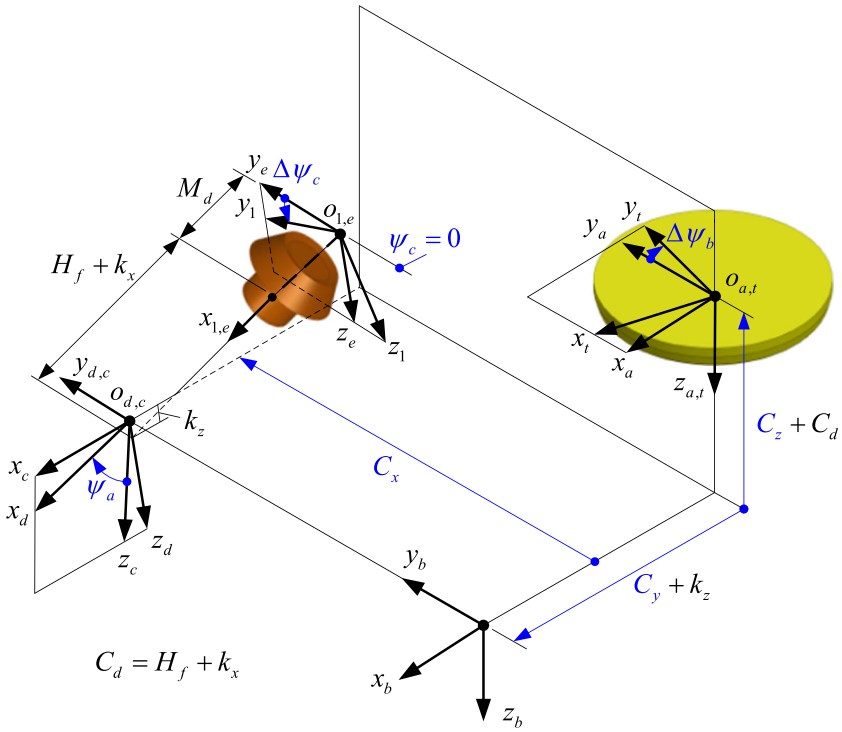

Fig. 4 Coordinate systems for bevel gear cutting on a trunnion table type five-axis machine

and the fillet center is

$$\begin{cases} x_{cf} = \rho_b \tan\left(\pi/4 - \alpha_b/2\right) \\ z_{cf} = -\rho_b \end{cases}$$

where u is a curve parameter and symbol ± indicates the inner and outer blade edges, respectively. The position vector of the blade edge may be represented in the tool coordinate system S_t using the following homogeneous coordinates:

$$\mathbf{r}_t(u,\beta) = [\,(x_a + r_0)\cos\beta \quad (x_a + r_0)\sin\beta \quad z_a \quad 1\,]^T \qquad (2)$$

Table 1 Basic and manufacturing parameters for the example pair

		Pinion		Ring gear	
Items		Convex	Concave	Convex	Concave
(A) Basic gear data					
Number of teeth	z	16		33	
Outer module	m_{et}	3.500			
Pressure angle	α_n	20.000°			
Spiral angle	β_m	35.000° L.H.		35.000° R.H.	
(B) Gear blank data					
Pitch angle	δ	25.866°		64.133°	
Face angle	δ_a	30.727°		66.464°	
Outer diameter	d_{ae}	63.408		117.221	
Outer whole depth	h_e	6.869		6.869	
Face width	b	19.500		19.500	
Mounting distance	M_d	75.000		36.000	
(C) Assembly data					
Shaft angle	Σ	90.000°			
Offset	V	0.000		–	
Axial setting	H	0.000		0.000	
(D) Cutter data					
Profile angle	α_b	24°	16°	24°	16°
Cutter radius	r_0	54.250	55.750	54.250	55.750
Fillet radius	ρ_b	0.700	0.700	0.700	0.700
(F) Five-axis machine tool					
Offset along x_d	k_x	0.085			
Offset along z_d	k_z	0.06			
Fixture height (measured)	H_t	140.408		97.826	

Table 2 Universal cradle type machine settings for the example pair

Items		Pinion		Gear	
		Convex	Concave	Convex	Concave
Tilt angle	i	1.106°		0.995°	
Swivel angle	j	28.332°		−67.396°	
Initial cradle angle setting	θ_c	64.598°		−63.349°	
Radial setting	S_R	50.171		50.234	
Vertical offset	E_m	−0.236		0.000	
Increment of machine center to back	ΔA	−0.332		−0.459	
Sliding base feed setting	ΔB	0.965–2.910ϕ_c		2.399	
Machine root angle	γ_m	21.339°		58.508°	
Roll ratio	R_a	2.27513		1.10112	

According to the literature [10], the virtual cradle type machine has nine machine settings: (1) the tilted angle i, (2) the swivel angle j, (3) the radial distance S_R, (4) the initial cradle angle setting θ_c, (5) the vertical offset E_m, (6) the sliding base ΔB, (7) the machine root angle γ_m, (8) the increment of machine center to back ΔA, and (9) the roll ratio R_a (see Fig. 3). All these can be determined by the calculation formulas provided by the machine manufacturers. Two other settings move the machine axes for positioning the tool and work gear to enable the generating process and flank modification for bevel gear production: parameter ϕ_1, the work gear rotation angle; and parameter ϕ_c, the cradle rotation angle.

As Fig. 2 shows, coordinate systems S_t and S_1 are fixedly connected to the cutting tool and work gear, respectively. S_a and S_f are auxiliary coordinate systems for the cutting positions and motions of the tool and work gear. The transformation matrix from S_t to S_1 yields the locus of the tool in the work gear coordinate system whose position vector is represented in Eq. (3). The envelope for a one-parameter family of surfaces generates the bevel gear tooth surface, which can be determined from the equation of meshing [10] and two boundary conditions of gear blank.

$$\mathbf{r}_1^{(U)}(u,\beta,\phi_c) = \mathbf{M}_{1f}^{(U)}(\phi_1)\mathbf{M}_{\mathrm{ft}}^{(U)}(i,j,S_R,\theta_c,E_m,\Delta B,\gamma_{\mathrm{m}},\Delta A,\phi_c)\mathbf{r}_t(u,\beta) \tag{3}$$

Here, the transformation matrices from S_t to S_1 for the cradle type machine are

$$\mathbf{M}_{1f}^{(U)}(\phi_1) = \begin{bmatrix} 1 & 0 & 0 & 0 \\ 0 & \cos\phi_1 & -\sin\phi_1 & 0 \\ 0 & \sin\phi_1 & \cos\phi_1 & 0 \\ 0 & 0 & 0 & 1 \end{bmatrix}$$

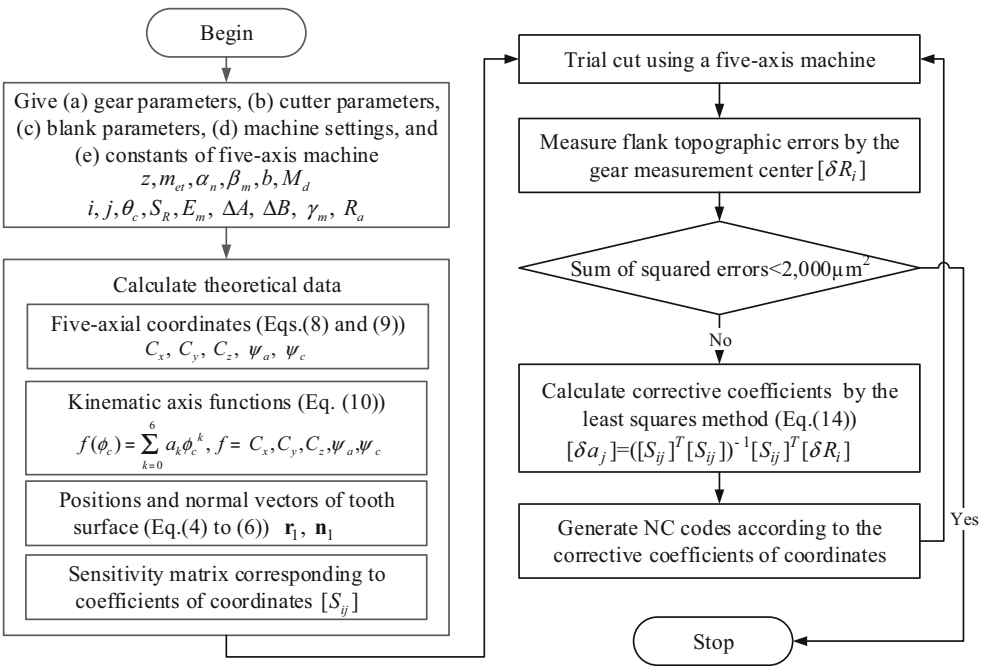

Fig. 5 Flow chart of flank correction method for a five-axis machine

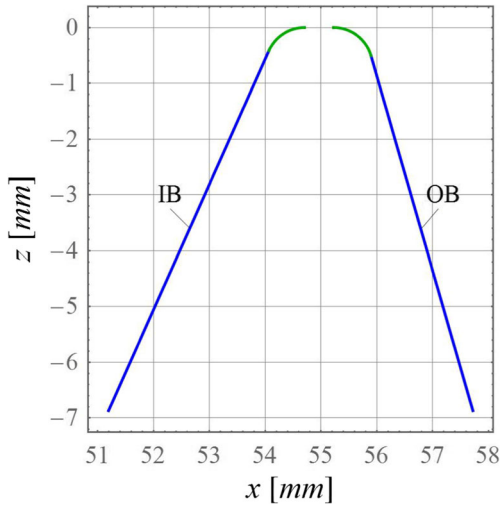

Fig. 6 Positions of the cutting edges for both gears

and

$$\mathbf{M}_{\mathrm{ft}}^{(U)}(\phi_c) = \begin{bmatrix} \cos\gamma_m & 0 & \sin\gamma_m & -\Delta A \\ 0 & 1 & 0 & 0 \\ -\sin\gamma_m & 0 & \cos\gamma_m & 0 \\ 0 & 0 & 0 & 1 \end{bmatrix} \begin{bmatrix} 1 & 0 & 0 & 0 \\ 0 & 1 & 0 & E_m \\ 0 & 0 & 1 & -\Delta B \\ 0 & 0 & 0 & 1 \end{bmatrix}$$
$$\begin{bmatrix} \cos(\theta_c+\phi_c) & \sin(\theta_c+\phi_c) & 0 & 0 \\ -\sin(\theta_c+\phi_c) & \cos(\theta_c+\phi_c) & 0 & 0 \\ 0 & 0 & 1 & 0 \\ 0 & 0 & 0 & 1 \end{bmatrix} \begin{bmatrix} -\sin j & -\cos j & 0 & S_R \\ \cos j & -\sin j & 0 & 0 \\ 0 & 0 & 1 & 0 \\ 0 & 0 & 0 & 1 \end{bmatrix} \begin{bmatrix} \cos i & 0 & \sin i & 0 \\ 0 & 1 & 0 & 0 \\ -\sin i & 0 & \cos i & 0 \\ 0 & 0 & 0 & 1 \end{bmatrix}$$

3 Mathematical model based on a trunnion table type five-axis machine

Because the trunnion-table and rotary-table-swivel-head types of five-axis machines include a rotary table, they are very suitable for machining gear tooth surfaces. The first is therefore used as an example in this paper. In this trunnion table type machine, coordinate systems S_t and S_1 are rigidly connected to the cutting tool and work gear, respectively (see Fig. 4), and S_a and S_e are the auxiliary coordinate systems for the movement of the five axes. C_x, C_y, and C_z are the three coordinates for translating the axes, and ψ_a and ψ_c are the coordinates for the workpiece rotation angle and table tilting angle, respectively. These five coordinates are moved synchronously by a CNC controller so as to satisfy the movement requirement for cutting bevel gears. An additional coordinate, ψ_b, is the angle for tool rotation, while $\Delta\psi_b$ and $\Delta\psi_c$ are the incremental angles for tool rotation and work gear rotation, respectively. Parameter H_f is the fixture height, and parameters k_x and k_z are machine constants, the former representing the distance between the table datum plane and the table tilting axis y_c, and the latter, the offset between axes y_c and x_e. Each of these must be measured out before cutting.

The bevel gear tooth surface is generated by an envelope of a family of tool surfaces $\mathbf{r}_t$ whose position vector is derived using the following coordinate transformation:

$$\mathbf{r}_1(u,\beta,\phi_c) = \mathbf{M}_{1e}(\phi_1)\mathbf{M}_{et}\left(\psi_a,\Delta\psi_b,\Delta\psi_c,C_x,C_y,C_z\right)\mathbf{r}_t(u,\beta) \quad (4)$$

where the transformation matrices from S_t to S_1 for the five-axis machine are

$$\mathbf{M}_{1e}(\phi_1) = \begin{bmatrix} 1 & 0 & 0 & 0 \\ 0 & \cos\phi_1 & \sin\phi_1 & 0 \\ 0 & -\sin\phi_1 & \cos\phi_1 & 0 \\ 0 & 0 & 0 & 1 \end{bmatrix}$$

and

$$\mathbf{M}_{et}(\phi_c)=\begin{bmatrix}1&0&0&0\\0&-\cos\Delta\psi_c&-\sin\Delta\psi_c&0\\0&\sin\Delta\psi_c&-\cos\Delta\psi_c&0\\0&0&0&1\end{bmatrix}\begin{bmatrix}1&0&0&M_d+H_f+k_x\\0&1&0&0\\0&0&1&k_z\\0&0&0&1\end{bmatrix}\begin{bmatrix}\sin\psi_a&0&\cos\psi_a&0\\0&1&0&0\\-\cos\psi_a&0&\sin\psi_a&0\\0&0&0&1\end{bmatrix}$$
$$\begin{bmatrix}1&0&0&0\\0&1&0&-C_x\\0&0&1&0\\0&0&0&1\end{bmatrix}\begin{bmatrix}1&0&0&-(C_y+k_z)\\0&1&0&0\\0&0&1&-(C_z+H_f+k_x)\\0&0&0&1\end{bmatrix}\begin{bmatrix}\cos\Delta\psi_b&-\sin\Delta\psi_b&0&0\\\sin\Delta\psi_b&\cos\Delta\psi_b&0&0\\0&0&1&0\\0&0&0&1\end{bmatrix}$$

The five coordinates for cutting are functions of the cradle angle ϕ_c, which in cradle type machines dominates the generating position, while the workpiece rotation angle ϕ_1 is equal to $R_a\phi_c$ where R_a is the roll ratio. The position vector $\mathbf{r}_1$ is derived as a function of three variables: u, β, and ϕ_c The first two are variables of the cutter surface, while the last is its motion parameter. According to differential geometry, a normal vector $\mathbf{n}_1$ to a surface is obtained by taking the cross-product at a surface point of the two tangent vectors that are partial derivatives of $\mathbf{r}_1$ with respect to u and β. Relative velocity $\mathbf{v}_1^{(1t)}$ is then a time differential of $\mathbf{r}_1$, while the motion parameter ϕ_c is a function of time. These variables are calculated as follows:

$$\begin{cases}\mathbf{n}_1(u,\beta,\phi_c)=\dfrac{\dfrac{\partial\mathbf{r}_1(u,\beta,\phi_c)}{\partial u}\times\dfrac{\partial\mathbf{r}_1(u,\beta,\phi_c)}{\partial\beta}}{\left\|\dfrac{\partial\mathbf{r}_1(u,\beta,\phi_c)}{\partial u}\times\dfrac{\partial\mathbf{r}_1(u,\beta,\phi_c)}{\partial\beta}\right\|}\\ \mathbf{v}_1^{(1t)}(u,\beta,\phi_c)=\dfrac{\partial\mathbf{r}_1(u,\beta,\phi_c)}{\partial\phi_c}\dot{\phi}_c\end{cases}\tag{5}$$

The topographic points of the tooth surface can then be solved using an equation of meshing (Eq. (6)), derived when the relative velocity is perpendicular to the normal vector, together with two boundary conditions of the gear blank:

$$f_1(u,\beta,\phi_c)=\mathbf{n}_1(u,\beta,\phi_c)\cdot\mathbf{v}_1^{(1t)}(u,\beta,\phi_c)=0\tag{6}$$

4 Derivation of the five-axis coordinates

If different machines are employed to produce the same gear using the same tool, the relative motions between the tool and the work gear should be identical. In other words, the coordinate transformation matrix of the five-axis machine should equal that of the cradle type machine so that the following relation is satisfied:

$$\begin{aligned}&\mathbf{M}_{et}(\psi_a,\Delta\psi_b,\Delta\psi_c,C_x,C_y,C_z)\\&=\mathbf{M}_{\mathrm{ft}}^{(U)}(i,j,S_R,\theta_c,E_m,\Delta B,\gamma_{\mathrm{m}},\Delta A,\phi_c)\\&=\begin{bmatrix}e_{11}&e_{12}&e_{13}&e_{14}\\e_{21}&e_{22}&e_{23}&e_{24}\\e_{31}&e_{32}&e_{33}&e_{34}\\0&0&0&1\end{bmatrix}\end{aligned}\tag{7}$$

According to inverse kinematics, six coordinates (including the tool rotation angle) can be determined by equating the elements in the above two matrices:

$$\begin{cases}\psi_a(\phi_c)=-\cos^{-1}(e_{13})\\ \Delta\psi_b(\phi_c)=\tan^{-1}(x,y)=\tan^{-1}(-e_{11},e_{12})\,,\\ \Delta\psi_c(\phi_c)=\tan^{-1}(e_{33},e_{23})\end{cases}\quad\begin{cases}C_x(\phi_c)=e_{24}\cos\Delta\psi_c-e_{34}\sin\Delta\psi_c\\ C_y(\phi_c)=D\sin\psi_a-E\cos\psi_a-k_z\\ C_z(\phi_c)=E\sin\psi_a+D\cos\psi_a-H_f-k_x\end{cases}\tag{8}$$

where

$$\begin{cases}D=-e_{14}+H_f+k_x+M_d\\ E=e_{24}\sin\Delta\psi_c+e_{34}\cos\Delta\psi_c+k_z\end{cases}$$

Here, the incremental angles $\Delta\psi_b$ can be ignored because they have no influence on the tooth geometry, but the incremental angles $\Delta\psi_c$ must be added into the workpiece rotation angle as

$$\psi_c(\phi_c)=-\phi_1+\Delta\psi_c=-R_a\phi_c+\Delta\psi_c(\phi_c)\tag{9}$$

Because the five coordinates are functions of the cradle angle ϕ_c, each coordinate can be further approximated by the Maclaurin series below. Degree six is usually assumed to meet the requirement of machining accuracy:

$$\begin{cases}f(\phi_c)=\sum\limits_{k=0}^{n}\dfrac{f^{(k)}(0)\cdot{\phi_c}^k}{k!}+R^{(n)}(\phi_c)\approx\sum\limits_{k=0}^{6}a_k{\phi_c}^k\\ f=C_x,C_y,C_z,\psi_a,\psi_c\end{cases}\tag{10}$$

Table 3 Theoretical five-axis coordinates for the finishing cutting positions of the pinion and gear

	Pinion		Gear	
Coordinate	Convex	Concave	Convex	Concave
ϕ_c cradle angle (rad)	$+0.334 \geq \phi_c \geq -0.349$		$-0.290 \leq \phi_c \leq +0.312$	
C_x x-axis	$-45.4031-21.9571\phi_c+22.7437\phi_c^2$ $+3.8708\phi_c^3-1.9085\phi_c^4-0.2360\phi_c^5+0.0638\phi_c^6$		$+45.5517-21.2752\phi_c-23.1263\phi_c^2$ $+2.8978\phi_c^3+2.0644\phi_c^4-0.0078\phi_c^5-0.0792\phi_c^6$	
C_y y-axis	$-177.7720-44.1399\phi_c-11.6318\phi_c^2$ $+7.3729\phi_c^3+1.0702\phi_c^4-0.3677\phi_c^5-0.0500\phi_c^6$		$-48.0294+47.5630\phi_c-10.0315\phi_c^2$ $-8.2338\phi_c^3+0.4945\phi_c^4+0.4573\phi_c^5+0.0324\phi_c^6$	
C_z z-axis	$-58.5513+0.2085\phi_c-1.1464\phi_c^2$ $-0.5196\phi_c^3+0.0955\phi_c^4+0.0260\phi_c^5-0.0032\phi_c^6$		$+18.4622+1.2014\phi_c-0.0425\phi_c^2$ $-0.2002\phi_c^3+0.0035\phi_c^4+0.0100\phi_c^5-0.0001\phi_c^6$	
ψ_a table tilting angle	$-68.0091+0.8960\phi_c-0.3258\phi_c^2$ $-0.1514\phi_c^3+0.0268\phi_c^4+0.0080\phi_c^5-0.0008\phi_c^6$		$-31.4362+0.9944\phi_c-0.0211\phi_c^2$ $-0.1663\phi_c^3-0.0018\phi_c^4+0.0083\phi_c^5+0.0005\phi_c^6$	
ψ_c work angle	$+0.9620-131.0551\phi_c-0.4875\phi_c^2$ $+0.1151\phi_c^3+0.0428\phi_c^4-0.0054\phi_c^5-0.0017\phi_c^6$		$+1.9040-63.1702\phi_c-0.9555\phi_c^2$ $-0.0136\phi_c^3-0.0799\phi_c^4+0.0061\phi_c^5-0.0024\phi_c^6$	

The polynomial coefficients can then be modulated for flank correction.

5 Flank correction on a five-axis machine

Because manufacturing deviations of the gear tooth surfaces are caused primarily by cutter and machine axes errors, the flank geometry of a bevel gear has a dominant influence on contact performance, and the gear's flank deviations must be reduced as much as possible. The flank correction method for a bevel gear based on a cradle type machine, explained in Ref. [9], is well developed and has been applied on a CNC bevel gear cutting machine [10] but never on a five-axis machine. The main procedures in this method are (1) measuring the flank topographic errors using a coordinate measuring machine (CMM), (2) calculating the sensitivity matrix of the machine settings with regard to variations in the flank topographic points, and (3) determining the corrective machine settings based on the sensitivity matrix and the flank topographic errors. More specifically, these corrective settings are measured using the least squares method as shown in the following equations.

The generated tooth surface can be represented as a function of variables (u, β) and the polynomial coefficients a_j of the five-axis motion. It may be expressed as

$$\mathbf{r}_1 = \mathbf{r}_1(u, \beta, a_j) \quad (j = 1, \ldots, q) \tag{11}$$

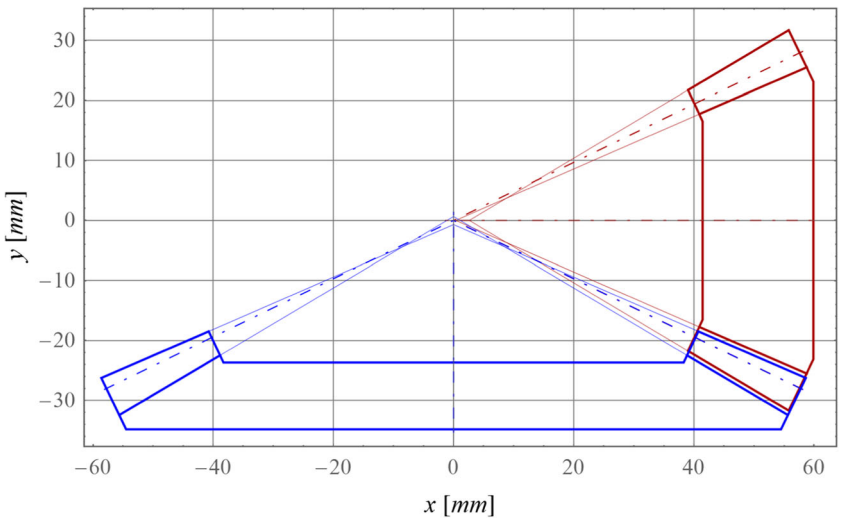

Fig. 7 Gear blanks for the gear pair

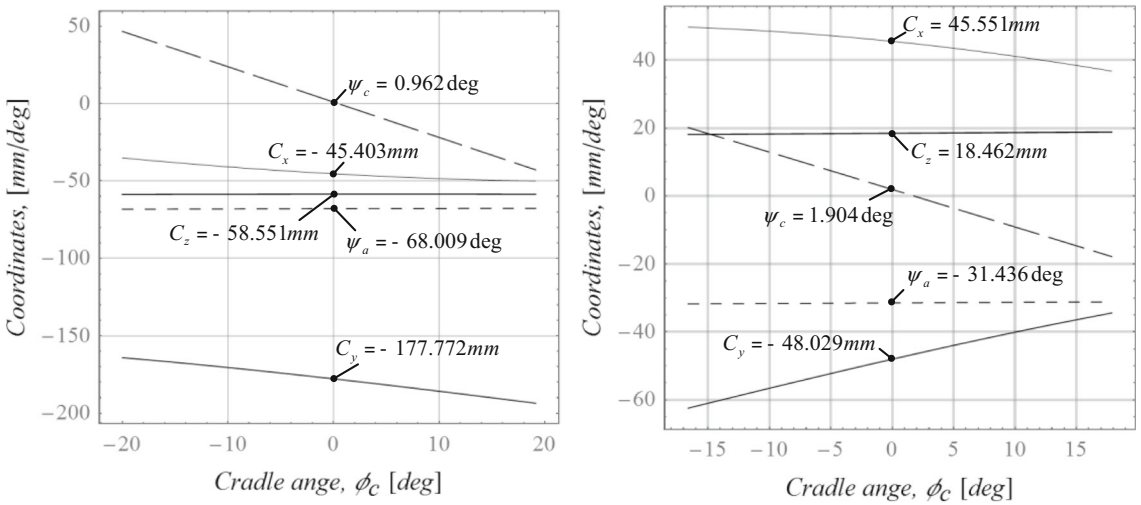

(a) Pinion (b) Gear

Fig. 8 Theoretical kinematic relations of the five-axis coordinates for the pinion and gear

where q is the number of polynomial coefficients which equals to 6×7. According to differential geometry, the surface variation vector is as follows:

$$\delta \mathbf{r}_1 = \frac{\partial \mathbf{r}_1}{\partial u}\delta u + \frac{\partial \mathbf{r}_1}{\partial \beta}\delta \beta + \sum_{j=1}^{q} \frac{\partial \mathbf{r}_1}{\partial a_j}\delta a_j \tag{12}$$

Because tangent vectors $\frac{\partial \mathbf{r}_1}{\partial u}$ and $\frac{\partial \mathbf{r}_1}{\partial \beta}$ are both perpendicular to the surface normal, taking the inner product of both sides of the above equation with the surface normal $\mathbf{n}_1$ yields the following normal surface variation:

$$\begin{aligned} \delta \mathbf{r}_1 \cdot \mathbf{n}_1 &= \left(\frac{\partial \mathbf{r}_1}{\partial u}\delta u + \frac{\partial \mathbf{r}_1}{\partial \beta}\delta \beta + \sum_{j=1}^{q} \frac{\partial \mathbf{r}_1}{\partial a_j}\delta a_j \right) \cdot \mathbf{n}_1 \\ &= \sum_{j=1}^{q} \left(\frac{\partial \mathbf{r}_1 \cdot \mathbf{n}_1}{\partial a_j} \right) \delta a_j \end{aligned} \tag{13}$$

The corrections $[\delta a_j]$ for coefficients can be further derived as

$$[\delta a_j] = \left([S_{ij}]^T [S_{ij}] \right)^{-1} [S_{ij}]^T [\delta R_i] \tag{14}$$

where $[S_{ij}]$ is the sensitivity matrix and $[\delta R_i]$ is the flank topographic errors.

Figure 5 illustrates this method applied in this paper as a flow chart. First, based on the given settings for the cradle type machine, the five-axis coordinates are derived and represented as polynomial approximations. Next, the positions and normal vectors of the topographic points of the tooth surface are calculated, and the effect on these points of a small variation (0.01) in each of the five axes' polynomial coefficients is evaluated to produce the sensitivity matrix. A five-axis machine is then adopted for gear production, and its flank topographic errors are derived using a gear measurement center. If the sum of squared errors of the work gear is larger than 2000 μm^2, a correction must be performed. The corrective coefficients are also determined using the least squares method based on the measured errors and sensitivity matrix. This process allows generation of the corrective NC codes to reduce manufacturing errors in the subsequent production of a work gear.

6 Numerical examples for an FM bevel gear produced by a five-axis machine

The numerical example is based on an FM spiral bevel gear pair whose pinion and gear are produced by the duplex helical method, also called SGDH. This method employs a double-flank cut that enables very high productivity and uses the same cutting tool to produce both gears, meaning that the

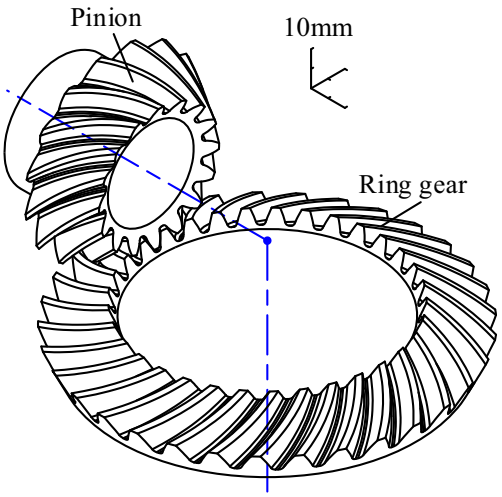

Fig. 9 3D models of the example pair (built using SolidWorks)

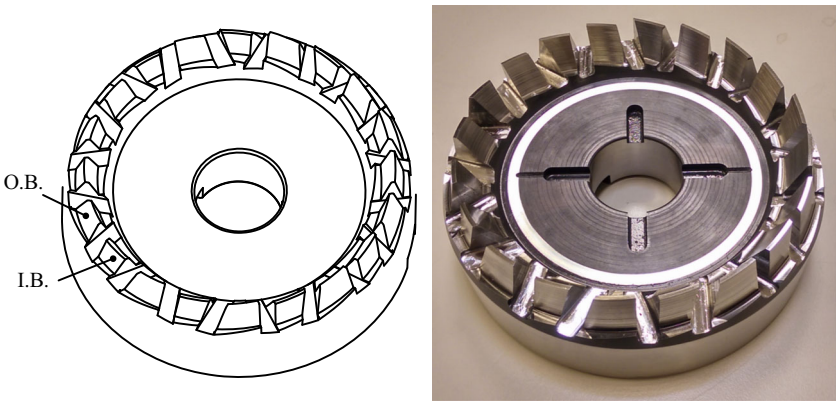

(a) 3D design (b) Cutter workpiece

Fig. 10 Solid cutter (designed and manufactured by the authors)

convex and concave flanks of the tooth surface are cut simultaneously. The basic gear parameters, manufacturing parameters, and machine settings of the cradle type machine are listed in Tables 1 and 2, respectively. Except for the given parameters and those for the five-axis machine, all these are calculated based on the machine summary provided by Gleason [11]. Based on the machine settings, both gears are produced using a generating motion, with a helical motion of the sliding base applied only for flank modification of the pinion. As illustrated in Figs. 6 and 7, respectively, the profile angle of the inner edge is larger than that of the outer edge and the gear blanks have tapered depth teeth in the assembly position.

Substituting the universal machine settings, the machine constants of the five-axis machine, and the fixture height into Eqs. (8) and (9) determines the five coordinates for the cutting positions. The theoretical five-axis coordinates are functions of the cradle angle, which, based on Eq. (10), can be further approximated as polynomials of up to the sixth degree (see Table 3). Figure 8 then shows their kinematic relation, with cradle angle ϕ_c ranging from +19.1 to −20.0deg and from −16.6 to +17.9degfor the pinion and gear, respectively. These settings enable a generating motion from the toe to the heel of the tooth surface. The functions of the five coordinates and the cutter parameters are then substituted into Eqs. (1), (2), (4), and (5) to yield the position and normal vectors of the work gear with three variables (u, β, ϕ_c). These variables are then solved using an equation of meshing (see Eq. (6)) and two boundary equations of the gear blank and substituted into Eqs. (4) and (5) to obtain the position and normal vectors of the topographic points. This process generates both the nominal data for gear measurement and the topographic points used to build the SolidWorks 3D models of the gear pair (see Fig. 9).

Table 4 Manufacturing errors of the cutter workpiece

Items		(a) Design	(b) Measurement	(c) Deviation
Profile angle	IB	24.000°	23.841°	−0.159°
	OB	16.000°	16.039°	+0.039°
Cutter radius	IB	54.250	54.376	+0.126
	OB	55.750	55.845	+0.095
Point width		1.500	1.469	−0.031

7 Experimental results for flank correction

The correctness of the proposed models is verified through several cutting experiments made on a trunnion table type five-axis machine equipped with a high precision Siemens 840D sl CNC controller with 5 μm repeatability. The experiments were performed using the specially designed and manufactured solid cutter (material SKH 55, HRC 62) shown in Fig. 10, whose workpiece was inspected using a CMM (see Table 4 for the manufacturing errors). This inspection identified profile angle errors for the inner and outer blades of −0.159 and +0.039deg, respectively, which directly affect

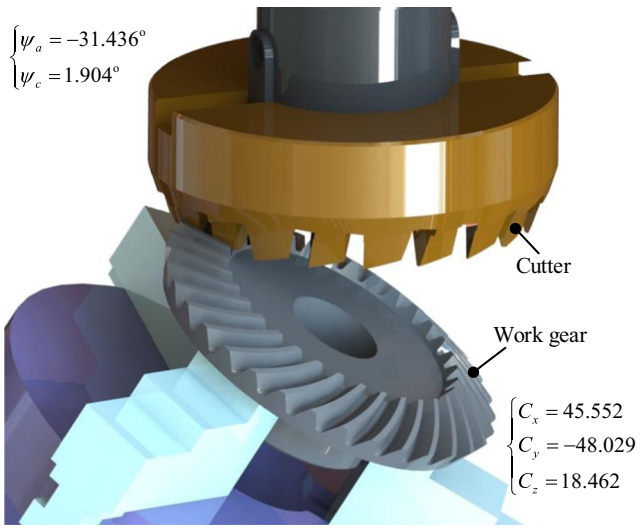

Fig. 11 Theoretical cutting position of the gear when $\phi_c = 0$ on the five-axis machine

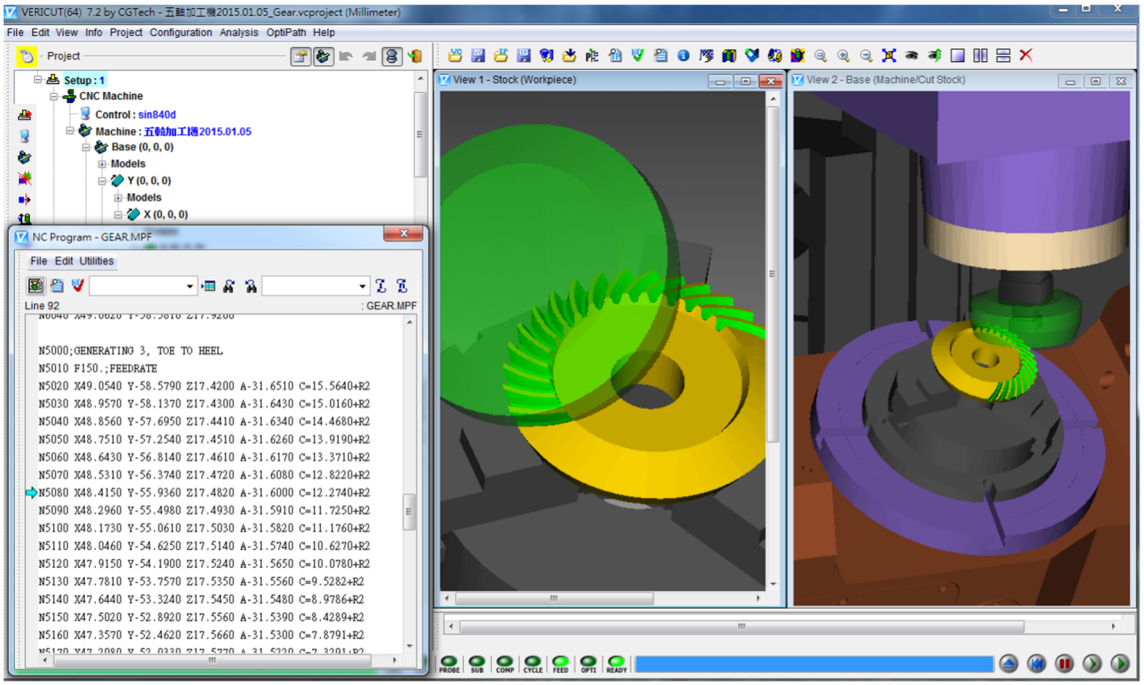

Fig. 12 Cutting simulation for the gear using VERICUT

the pressure angles of the convex and concave flanks of the bevel gear, respectively. The cutter radius errors, which influence the tooth flank curvatures, are +0.126 and +0.095 mm, and the point width error, which increases tooth thickness, is −0.031 mm.

Two operations are generally used in bevel gear cutting: a formate motion for roughing, which is enabled by setting ϕ_c to zero; and a generating motion for finishing, made possible by a range of ϕ_c. Before the cutting experiment, the NC codes for both gears are programmed according to the five-axis coordinates listed in Table 3 and tested for errors using the NC verification software VERICUT so as to prevent collisions and cutting mistake. To illustrate, Fig. 11 shows the cutting position for gear production when $\phi_c = 0$, with the corresponding cutting simulation illustrated in Fig. 12. After simulation, the finished workpiece is exported as an STL (StereoLithography) file whose left side is shown in Fig. 13. Here, the interpolation tolerance of STL file during VERICUT simulation is set to 0.05 mm. The flank topographic deviations between the STL and theoretic tooth surfaces are then evaluated using a program compiled by the authors. As Fig. 13 (right side) shows, the sum of the square is 2501 μm^2, and the tooth thickness error is +57 μm. These errors, which could be caused by simulation error, are small enough to confirm the correctness of the NC codes.

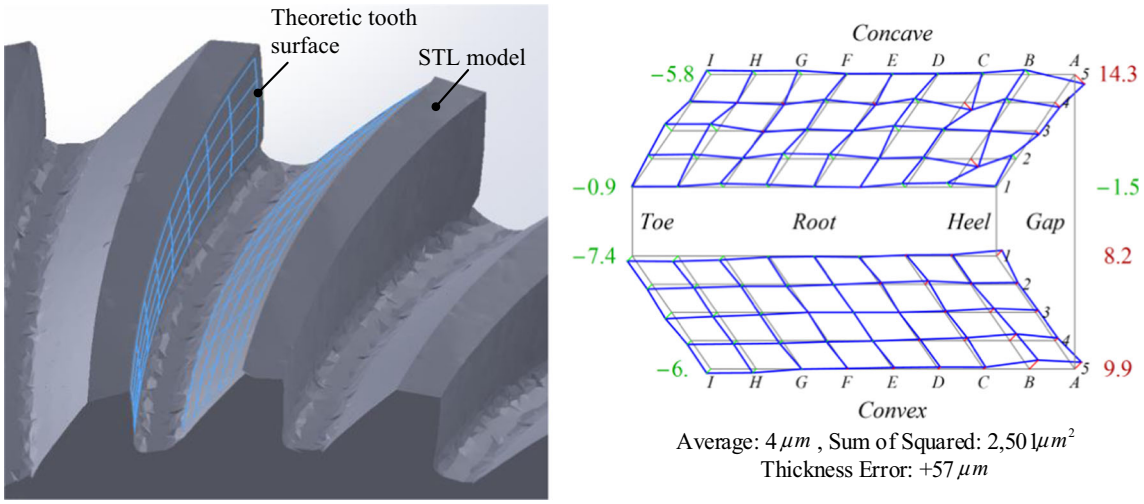

Fig. 13 Flank topographic deviations of the gear produced using VERICUT simulation before correction

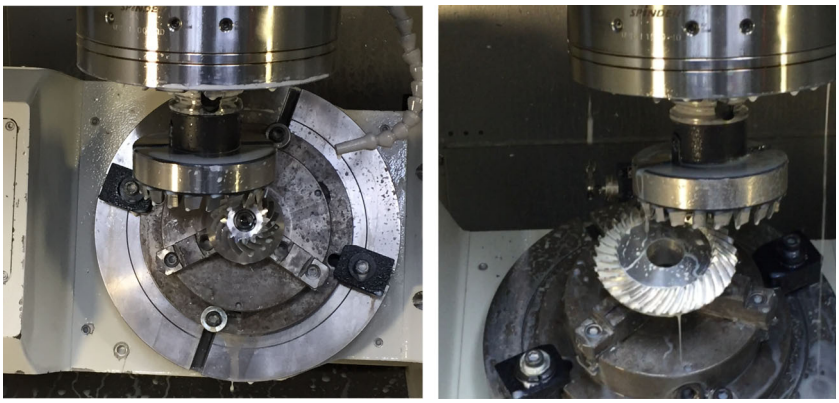

(a) Pinion (b) Gear

Fig. 14 Cutting the pinion and gear during the experiment

Figure 14 illustrates the cutting of the pinion and gear (material S20C) using the trunnion table type five-axis machine, which reveals the disadvantage of weak machining stiffness because of the large table tilting angle ($|\psi_a| > 45°$) for machining the pinion. The figure also shows the finished workpieces of both gears, which are then inspected using a Klingelnberg P40 gear measuring center. Before measurement, the nominal data [i.e., the basic data for the gear pair (MESINFO.CDS) and the positions and normal vectors of the topographic points (SOLL1.CDS)] are prepared and uploaded to the machine. Figure 15 shows the results: the sum of squares and tooth thickness error for the pinion are $10,077\ \mu m^2$ (for $2 \times 9 \times 5$points) and $-304\ \mu m$, respectively, and those for the gear are $10,266\ \mu m^2$ and $+19\ \mu m$.

Because the errors caused by cutter and machine axes errors are difficult to correct intuitively, a flank correction method is developed in which the cutter parameters and coordinate coefficients can be corrected together. However, only the latter is taken into account. Because of space constraints, however, this discussion considers only the coefficients as they apply to a gear. The first step is evaluation of the flank sensitivity topographies corresponding to the coefficients up to the sixth degree, exemplified in Figs. 16 and 17 by the zero and first degree coefficients, respectively. Because the cutter rotation angle ψ_b is a spindle axis, its coefficients have no influence on the tooth geometry. However, in the zero degree analysis, coefficients a_{x0} and a_{z0} affect the tooth geometry in the bias and lengthwise directions, coefficients a_{y0} and a_{a0} affect the profile angle, and all these coefficients together with coefficient a_{c0} affect the tooth thickness. In the first degree analysis, all the coefficients except coefficient a_{b1} have an effect in the bias direction. In total, 42 flank sensitivity topographies of the various coefficients make up the sensitivity matrix, which is partly illustrated in Fig. 18.

Based on this matrix, the proposed correction method can flexibly select which coefficients need to be corrected; for example, if the elements in the a_{c0} column are all equal to zero, then coefficient a_{c0} does not require correction. Such correction can be applied to both single- and double-flank cuts, although the former is likely to have a better outcome (in reducing manufacturing errors) than the latter because of its higher degrees of freedom. The single-flank correction is carried out by providing two sets of columns, one each for the inner and outer blade coefficients (see Fig. 18). The target topographic deviations for correction shown in Fig. 19a are determined based on the reverse of the gear errors measured

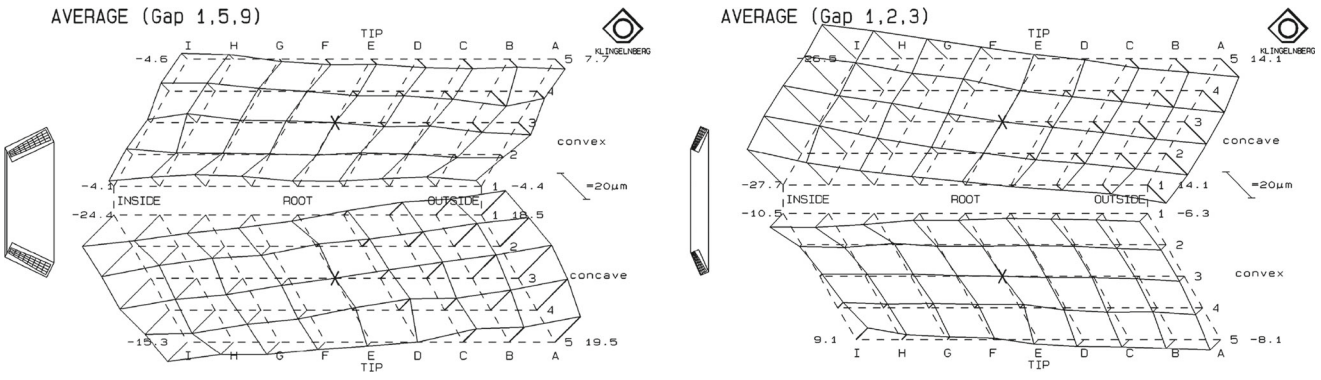

Sum of Squared: $10,077\mu m^2$, Thickness Error: - $304\mu m$

(a) Pinion

Sum of Squared: $10,266\mu m^2$, Thickness Error: +19μm

(b) Gear

Fig. 15 Flank topographic errors of the pinion and gear measured by the Klingelnberg P40 gear measuring center

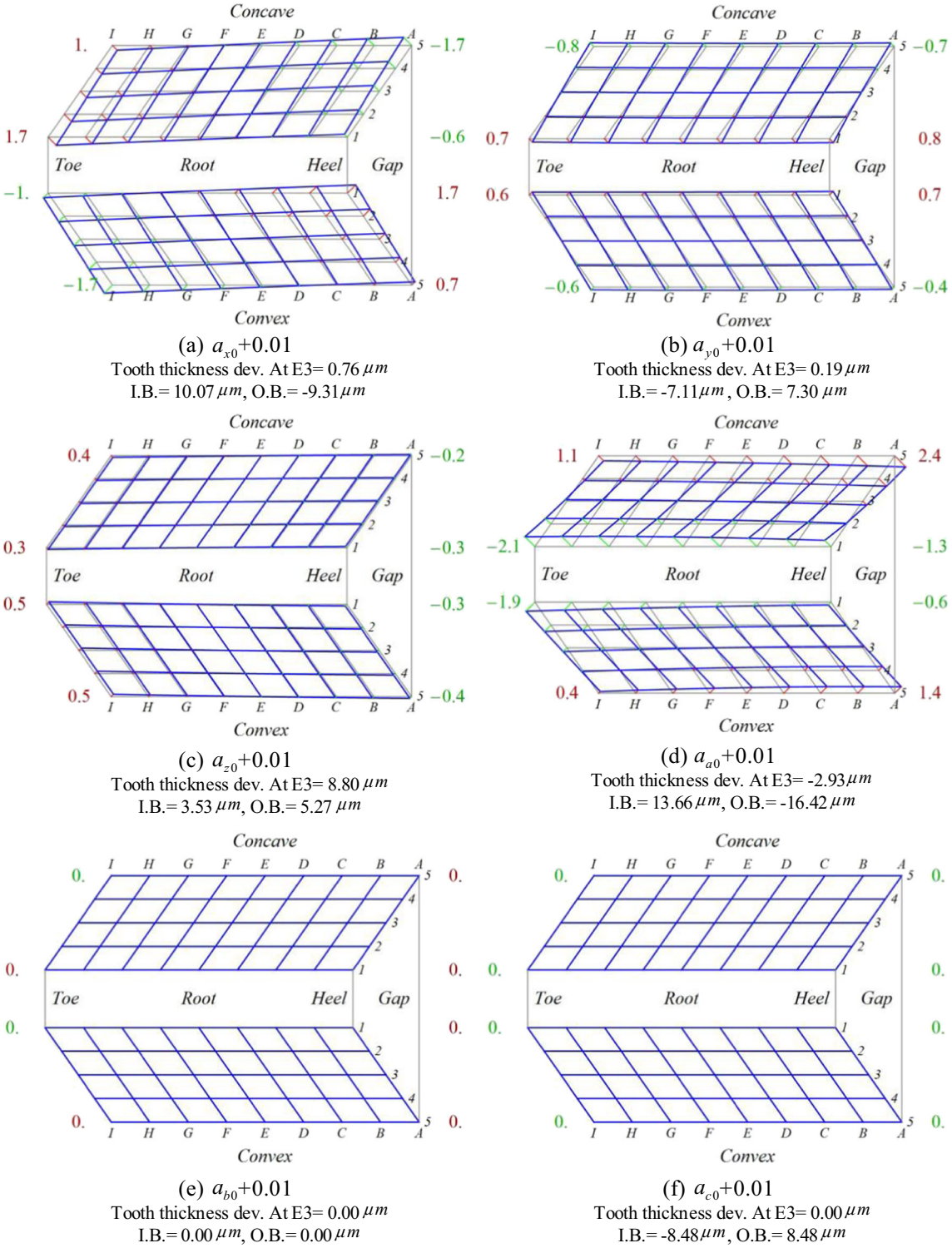

Fig. 16 Flank sensitivity topographies corresponding to the zero degree coefficients for the five-axis coordinates in a gear

(Fig. 15b). (Fig. 19b) shows the flank topographic errors after correction.The sensitivity matrix is applied here to correct a single-flank cut. The values of the matrix elements with regard to a_{a0} and a_{c0}, the coefficients of C_z, and the coefficients of the fifth and sixth degrees are zero, meaning that they are not involved in this correction under manufacturing conditions. The corrective coefficients are calculated using the least squares method based on the target flank deviations and given sensitivity matrix, which reduces the usual calculation time of about 14 min to less than a second (see Table 4 for the outcomes). The kinematic relations corresponding to the cradle angle are shown in Fig. 20.

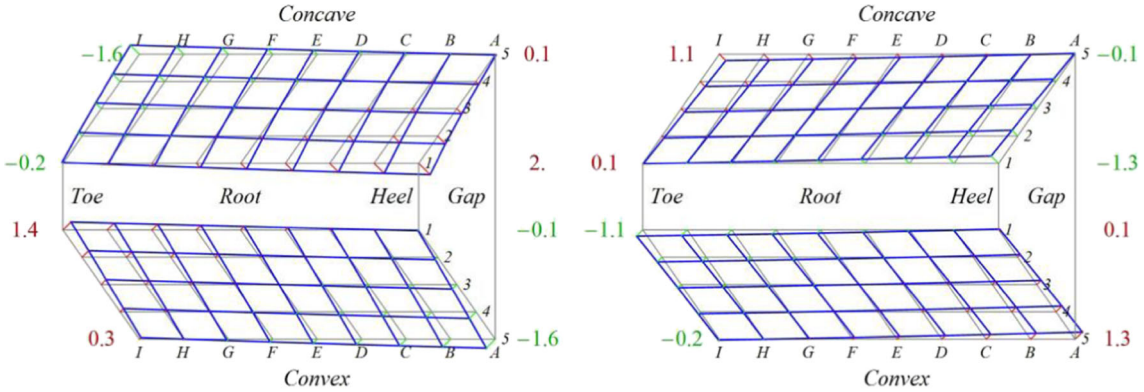

(a) a_{x1}+0.01
Tooth thickness dev. At E3= 0.02 μm
I.B.= 0.03 μm, O.B.= -0.01 μm

(b) a_{y1}+0.01
Tooth thickness dev. At E3= -0.03 μm
I.B.= -0.03 μm, O.B.= 0.00 μm

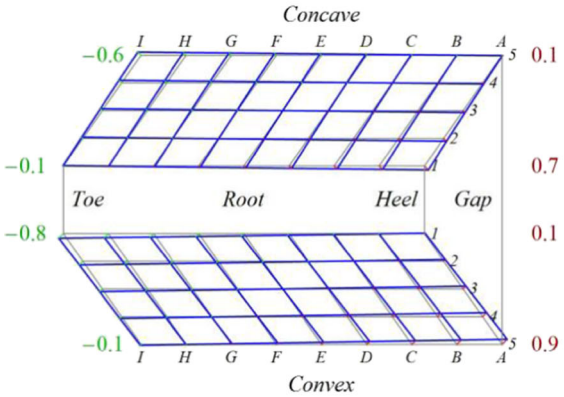

(c) a_{z1}+0.01
Tooth thickness dev. At E3= 0.01 μm
I.B.= 0.01 μm, O.B.= 0.00 μm

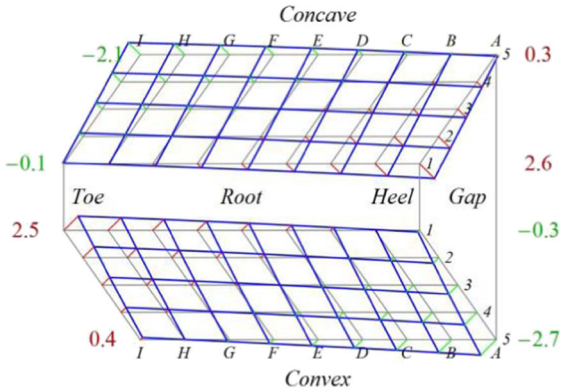

(d) a_{a1}+0.01
Tooth thickness dev. At E3= 0.02 μm
I.B.= 0.04 μm, O.B.= -0.02 μm

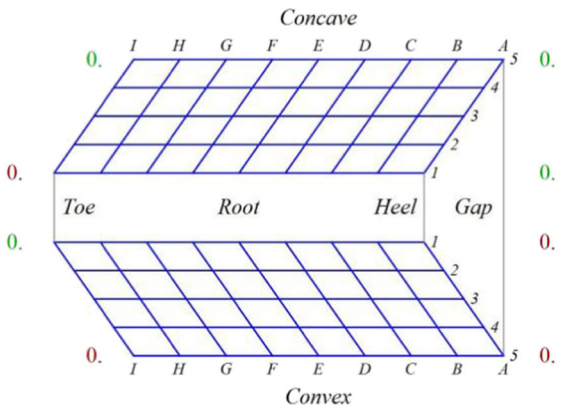

(e) a_{b1}+0.01
Tooth thickness dev. At E3= 0.00 μm
I.B.= 0.00 μm, O.B.= 0.00 μm

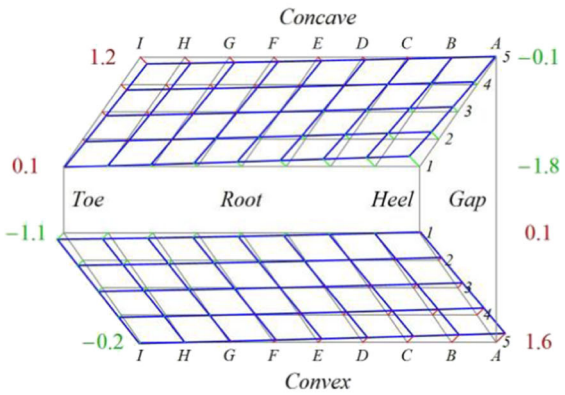

(f) a_{c0}+0.01
Tooth thickness dev. At E3= -0.03 μm
I.B.= -0.03 μm, O.B.= 0.00 μm

Fig. 17 Flank sensitivity topographies corresponding to the first degree coefficients for the five-axis coordinates in the gear

Once the errors are identified, the NC codes are generated anew and the new codes verified by VERICUT. The tooth surface deviations produced by the cutting simulation are pictured in Fig. 21, which shows them to have same tendency as the target (Fig. 19a). Hence, another cutting experiment is performed after the new correction program has been transferred to the CNC computer (Table 5). The experimental workpiece (the gear) displayed in Fig. 22 shows four sequential cuts, the first two produced by the original NC codes and the last two, by the corrected codes. Figure 23 then illustrates

Polynomial coefficients for the five-axis coordinates

		Inside blade					Outer blade					
		a_{x0}	a_{x1}	a_{x2}	…	a_{c5}	a_{c6}	a_{x0}	a_{x1}	a_{x2}	…	a_{c5}	a_{c6}
Topographical points	Convex flank	−0.09514	0.14198	−0.02776	…	−0.00940	0.00184	0	0	0	…	0	0
		−0.11552	0.11548	−0.01784	…	−0.00290	0.00045	0	0	0	…	0	0
		−0.13479	0.08735	−0.00993	…	−0.00063	0.00007	0	0	0	…	0	0
		−0.15280	0.05789	−0.00425	…	−0.00007	5.2×10^{-6}	0	0	0	…	0	0
		−0.16946	0.02741	−0.00093	…	-1.5×10^{-6}	5.1×10^{-8}	0	0	0	…	0	0
		⋮	⋮	⋮	⋱	⋮	⋮	⋮	⋮	⋮	⋱	⋮	⋮
		−0.60792	−0.22634	0.09728	…	−0.12863	−0.04468	0	0	0	…	0	0
	Concave flank	0	0	0	…	0	0	0.17285	−0.01612	0.00020	…	2.9×10^{-8}	-4.1×10^{-10}
		0	0	0	…	0	0	0.15300	−0.06189	0.00414	…	0.00006	-4.0×10^{-6}
		0	0	0	…	0	0	0.13433	−0.09950	0.01140	…	0.00076	−0.00009
		0	0	0	…	0	0	0.11657	−0.13127	0.02064	…	0.00353	−0.00057
		0	0	0	…	0	0	0.09956	−0.15855	0.03109	…	0.01041	−0.00208
		⋮	⋮	⋮	⋱	⋮	⋮	⋮	⋮	⋮	⋱	⋮	⋮
		0	0	0	…	0	0	−0.16885	0.01322	0.00037	…	-2.9×10^{-7}	-6.9×10^{-9}
Tooth thickness		−0.9311	−0.00074	-1.8×10^{-7}	…	0	0	0	0	0	…	0	0
		0	0	0	…	0	0	1.00693	0.00321	0.00001	…	-12.6×10^{-10}	-1.8×10^{-10}

Fig. 18 Part of the sensitivity matrix $[S_{ij}]$ for the polynomial coefficients of the five-axis coordinates

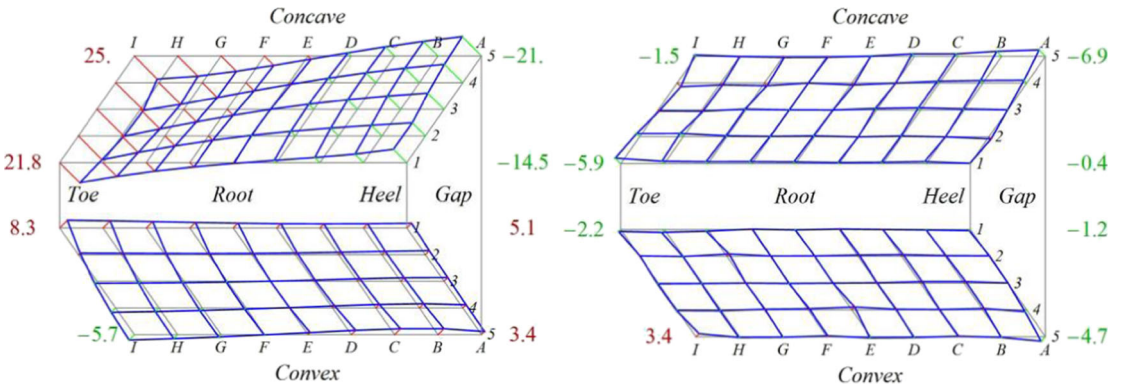

(a) Target of topographic deviations for correction (b) Flank topographic errors after correction

Fig. 19 Simulated flank topographic gear errors after correction

Fig. 20 Kinematic relations of the five-axis coordinates for the gear after correction

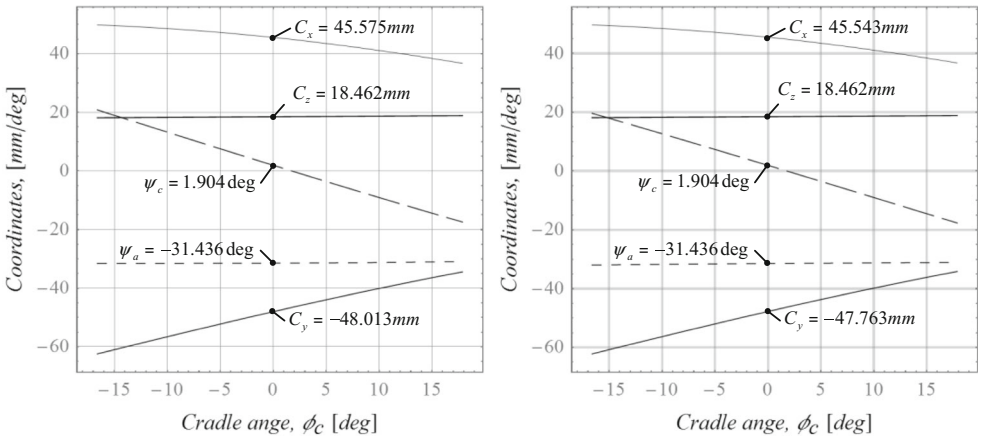

(a) Convex (b) Concave

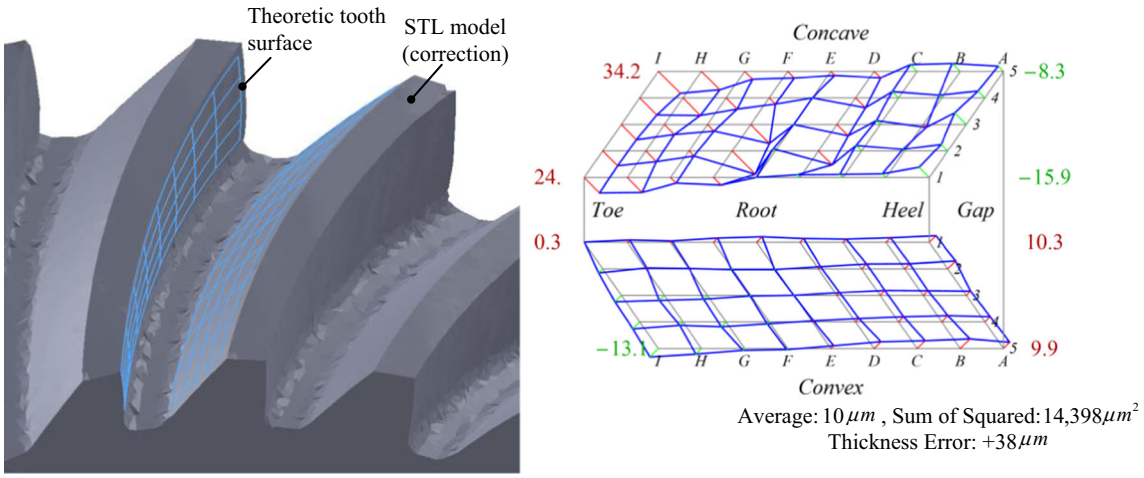

Fig. 21 Flank topographic deviations of the gear produced using VERICUT simulation after correction

Table 5 Corrective five-axis coordinates for the gear

Items	Convex	Concave
ϕ_c cradle angle (rad)	$-0.290 \le \phi_c \le +0.312$	
C_x x-axis	$+45.5754-21.5594\phi_c-23.0693\phi_c^2$ $+2.8845\phi_c^3+2.0652\phi_c^4-0.0078\phi_c^5+0.0792\phi_c^6$	$+45.5425-21.2726\phi_c-23.1194\phi_c^2$ $+2.8967\phi_c^3+2.0636\phi_c^4-0.0078\phi_c^5-0.0792\phi_c^6$
C_y y-axis	$-48.0132+47.4953\phi_c-10.0178\phi_c^2$ $-8.2375\phi_c^3+0.4946\phi_c^4+0.4573\phi_c^5+0.0324\phi_c^6$	$-47.7631+47.5792\phi_c-10.0284\phi_c^2$ $-8.2331\phi_c^3+0.4951\phi_c^4+0.4573\phi_c^5+0.0324\phi_c^6$
C_z z-axis	$+18.4622+1.2014\phi_c-0.0425\phi_c^2$ $-0.2002\phi_c^3+0.0035\phi_c^4+0.0100\phi_c^5-0.0001\phi_c^6$	$+18.4622+1.2014\phi_c-0.0425\phi_c^2$ $-0.2002\phi_c^3+0.0035\phi_c^4+0.0100\phi_c^5-0.0001\phi_c^6$
ψ_a machine root angle	$-31.4362+0.6420\phi_c+2.5108\phi_c^2$ $+4.7578\phi_c^3+0.8757\phi_c^4+0.0083\phi_c^5+0.0005\phi_c^6$	$-31.4362+1.3350\phi_c-0.7886\phi_c^2$ $+1.5643\phi_c^3-2.2501\phi_c^4+0.0083\phi_c^5+0.0005\phi_c^6$
ψ_c workpiece angle	$+1.9040-64.0887\phi_c+5.0144\phi_c^2$ $+3.9475\phi_c^3+0.1223\phi_c^4+0.0061\phi_c^5-0.0024\phi_c^6$	$+1.9040-62.3019\phi_c-3.3055\phi_c^2$ $+3.0086\phi_c^3+2.5581\phi_c^4+0.0061\phi_c^5-0.0024\phi_c^6$

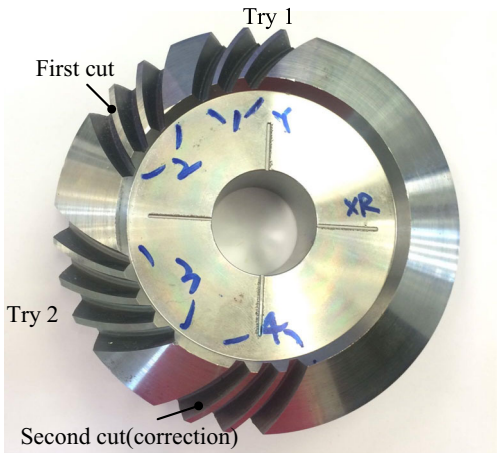

Fig. 22 The gear during flank correction

the outcome of using the corrective method: the maximum error is reduced from 27.7 to 8.6 μm, and the sum of squares is dramatically lowered from 10,266 to 1253 μm after just one round of correction. The tooth thickness error +8 μm can then be further eliminated by intuitively adjusting the workpiece rotation angle ψ_c.

8 Conclusions

In view of FM bevel gear manufacturing on a general five-axis machines is so much cheaper and more flexible than on a dedicated bevel gear cutting machine, especially in small-scale diverse production, this paper proposes a novel FM bevel gear flank correction method for a five-axis machine. The mathematical model of the tooth surface is established based on a trunnion-table type machine, after

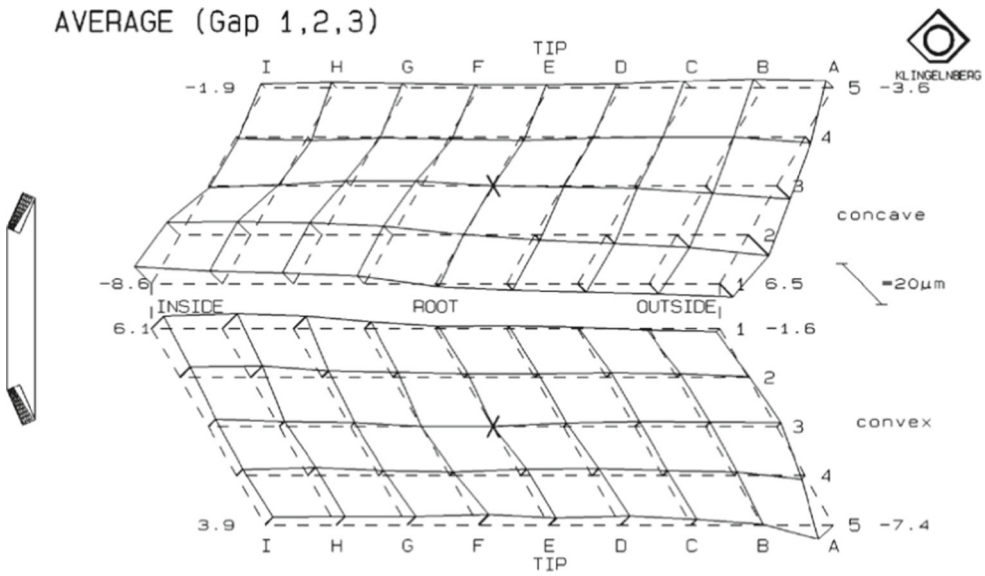

Fig. 23 Flank deviations of the gear after correction measured by the Klingelnberg P40 gear measuring center

which the five coordinates are derived from a virtual cradle type bevel gear cutting machine. Each coordinate is degenerated to a function of the generating angle and approximated as a polynomial in a Maclaurin series. The flank correction method itself is based on a sensitivity analysis that evaluates flank topographic deviations based on changes in these coordinate coefficients. That is, once the polynomial coefficients are adjusted, their corrections have been estimated using the least squares method based on the sensitivity matrix and the errors measured so as to reduce flank topographic errors. The correctness of the proposed method is verified in several cutting experiments using an SGDH gear pair as a numerical example. These verification results show that when applied to a gear, just one round of the new flank correction procedure effectively reduces the maximum error and sum of squares from 27.7 to 8.6 μm and from 10,266 to 1253 μm, respectively. Hence, even though the five-axis machine itself is subject to inherent errors of manufacturing, deformation, and assembly or large errors exist in the cutter, the proposed method can still be very effective in increasing its accuracy.

a_{x0}~a_{c6} i, j, θ_c, S_R, E_m, coefficients of the five-axis coordinates; $\Delta A, \Delta B, \gamma_m, R_a$, machine settings of the universal cradle type bevel gear cutting machine; r_0, cutter radius; u,β, parameters of the cutting surface; C_x, C_y, C_z, translating coordinates for the five-axis machine; $\mathbf{M}_{ij}$, homogeneous transformation matrix from coordinate system S_j to coordinate system S_i; $\mathbf{n}_1$, surface unit normal of the work gear in coordinate system S_1; $\mathbf{r}_1$, locus of the cutting tool in coordinate system S_1; $\mathbf{v}_1^{(1t)}$, relative velocity between the work gear and tool represented in coordinate system S_1; α_b, profile angle of the blade; ϕ_1, rotation angle of the work gear; ϕ_c, cradle rotation angle; ψ_a, ψ_c, rotation coordinates for the five-axis machine; ψ_b, spindle angle for the five-axis machine; $[S_{ij}]$, sensitivity matrix of the coefficients with regard to the flank topographic deviations; $[\delta a_j]$, corrections to the coefficients; $[\delta R_i]$, flank topographic deviations.

Acknowledgements The authors are grateful to the R.O.C.'s Ministry of Science and Technology for its financial support. Part of this work was performed under Contract No. MOST 104-2221-E-011-102. The authors also give special thanks to Dr. B.T. Sheen for his technical support in the cutting experiment.

References

1. Litvin FL, Gutman Y (1981) Methods of synthesis and analysis for hypoid gear-drives of "formate" and "helixform"—part 1. Calculations for machine settings for member gear manufacture of the formate and helixform hypoid gears. ASME J Mech Des 103 (1):83–88
2. Litvin FL, Gutman Y (1981) Methods of synthesis and analysis for hypoid gear-drives of "formate" and "helixform"—part 2. Machine setting calculations for the pinions of formate and helixform gears. ASME J. Mech. Des 103(1):89–101
3. Litvin FL, Gutman Y (1981) Methods of synthesis and analysis for hypoid gear-drives of "formate" and "helixform"—part 3. Analysis and optimal synthesis methods for mismatch gearing and its application for hypoid gears of "formate" and "helixform". ASME J. Mech. Des 103(1):102–110
4. Litvin FL, Zhang Y, Lundy M, Heine C (1988) Determination of settings of a tilted dead cutter for generation of hypoid and spiral bevel gears. J Mech, Trans, and Automation 110(4):495–500
5. Fong ZH (2000) Mathematical model of universal hypoid generator with supplemental kinematic flank correction motions. ASME J. Mech. Des. 122(1):136–142

6. Shih YP, Fong ZH, Lin GCY (2007) Mathematical model for a universal face hobbing hypoid gear generator. ASME J. Mech. Des. 129(1):38–47
7. Deng XZ, Li GG, Wei BY, Deng J (2014) Face-milling spiral bevel gear tooth surfaces by application of 5-axis CNC machine tool. Int J Adv Manuf Tech 71(5):1049–1057
8. Shih YP, Lai KL, Sun ZH, Yan XL (2015) Manufacture of face-milled spiral bevel gears on a five-axis CNC machine. Paper presented at the 14th IFToMM World Congress, October 25–30, 2015, Taipei, Taiwan, DOI: 10.6567/IFToMM.14TH.WC.OS6.032
9. Litvin FL, Fuentes A (2004) Gear geometry and applied theory, second edn. Cambridge University Press, Cambridge
10. Shih YP, Fong ZH (2008) Flank correction for spiral bevel and hypoid gears on a six-axis CNC hypoid generator. ASME J Mech Des 130(6):062604
11. Gleason Works, (1971) Calculation instructions: generated spiral bevel gears, duplex-helical method, including grinding, Rochester, NY